Multi-axial strength criterion of lightweight aggregate (LWA) concrete under the Unified Twin-shear strength theory

Li-cheng Wang*

State Key Laboratory of Coastal and Offshore Engineering, Dalian University of Technology, Dalian 116024, China

Abstract. The strength theory of concrete is significant to structure design and nonlinear finite element analysis of concrete structures because concrete utilized in engineering is usually subject to the action of multi-axial stress. Experimental results have revealed that lightweight aggregate (LWA) concrete exhibits plastic flow plateau under high compressive stress and most of the lightweight aggregates are crushed at this stage. For the purpose of safety, therefore, in the practical application the strength of LWA concrete at the plastic flow plateau stage should be regarded as the ultimate strength under multi-axial compressive stress state. With consideration of the strength criterion, the ultimate strength surface of LWA concrete under multi-axial stress intersects with the hydrostatic stress axis at two different points, which is completely different from that of the normal weight concrete as that the ultimate strength surface is open-ended. As a result, the strength criteria aimed at normal weight concrete do not fit LWA concrete. In the present paper, a multi-axial strength criterion for LWA concrete is proposed based on the Unified Twin-Shear Strength (UTSS) theory developed by Prof Yu (Yu *et al*. 1992), which takes into account the above strength characteristics of LWA under high compressive stress level. In this strength criterion model, the tensile and compressive meridians as well as the ultimate strength envelopes in deviatoric plane under different hydrostatic stress are established just in terms of a few characteristic stress states, i.e., the uniaxial tensile strength f_t, the uniaxial compressive strength f_c, and the equibiaxial compressive f_{bc}. The developed model was confirmed to agree well with experimental data under different stress ratios of LWA concrete.

Keywords: lightweight aggregate (LWA) concrete; Unified Twin-Shear Strength (UTSS) theory; multi-axial strength criterion; ultimate strength envelope; tensile and compressive meridians

1. Introduction

The structural concrete in practical project is generally subjected to the action of biaxial or triaxial stresses, i.e., under the complex stress states (Kupfer *et al*. 1969, Wang *et al*. 1987, Menetrey and Willam 1995, Imran and Pantazopoulou 1996). Experimental facts indicate that the concrete behavior under complex stress states is quite different from that under uniaxial loading, although currently the analysis and design methods of conventional reinforced concrete are generally based

*Corresponding author, Associate Professor, E-mail: wanglicheng2000@163.com

upon material properties obtained from the basic uniaxial strength test. However it is well known that the existence of realistic uniaxial conditions in structures is extremely rare (Leonard *et al*. 1991). Therefore, it will be very necessary that the strength of concrete should be investigated and represented under the complex stress states, which can, as a result, facilitate the rational design and trace realistically the structural response of the structures throughout their service life. Moreover, the wide use of computers and finite element method in design and analysis of reinforced concrete structures makes it desirable to establish a suitable and precise strength criterion.

In the past few decades, lots of strength criteria for concrete are developed independently, which can be clarified into three categories, i.e., the empirical criteria, physical category criteria and phenomenological criteria (Fan and Wang 2002). However, most of these criteria were constructed on the basis of empirical assumptions or experimental phenomena, but lack of the mechanical background. With consideration of the shortcomings of the available strength criteria, Prof. Yu proposed a new strength theory, namely the Unified Twin-Shear Strength (UTSS) theory, which was developed based on the orthogonal, octahedral twin-shear elements, as shown in Fig. 1 (Yu *et al*. 1992). In this theory, the maximum shear stress and the accompanying shear stresses are called principal shear stresses. The UTSS theory takes into account the effects of all independent stress components on two faces of the orthogonal, octahedral twin-shear element. In particular, a weighting coefficient *b* (ranging from 0 to 1) was introduced into the second principal stress and its corresponding normal stress to represent the relative effect of the second principal shear stress on the strength criterion (Fan and Wang 2002). This can efficiently overcome the shortage of Mohr-Coulomb model in which only the maximum shear stress and its corresponding normal stress are considered. Varying the *b* value between 0 and 1 makes it possible to embrace all envelopes between the two convex limit hexagons in the deviatoric plane, as depicted in Fig. 2. The advantages of the UTSS have been amply argued by Fan and Wang (2002).

Lightweight aggregate (LWA) concrete has been successfully used for structural purposes (tall buildings, long-span bridges, offshore platforms, and marine structures) because of its some excellent properties, for example the lower density and higher strength-to-weight ratio, as well as the fatigue resistance and the low permeability (Ergul *et al*. 2003, Melby *et al*. 1996, Haug and Fjeld 1996, Rossignolo *et al*. 2003, Song *et al*. 2000, Jo *et al*. 2007). It is increasingly recognized that for structural applications of LWA concrete, the density of concrete is often more important
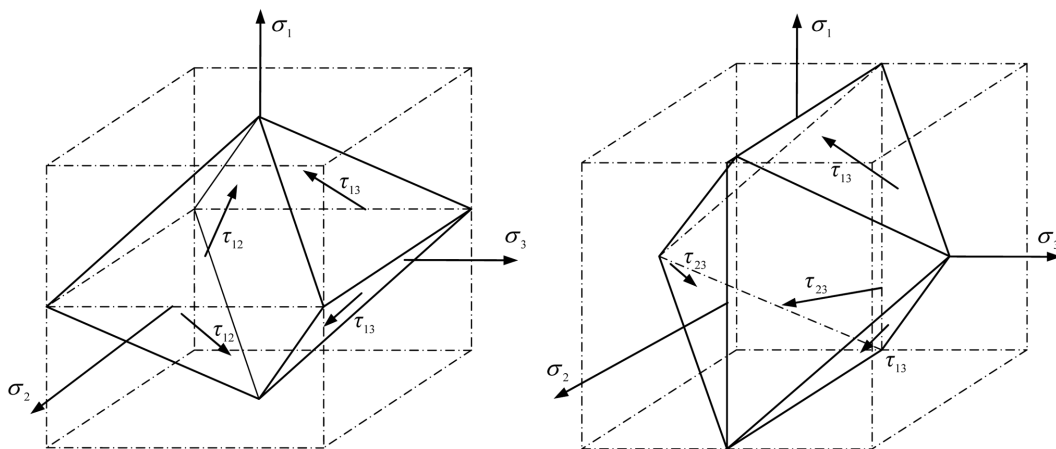

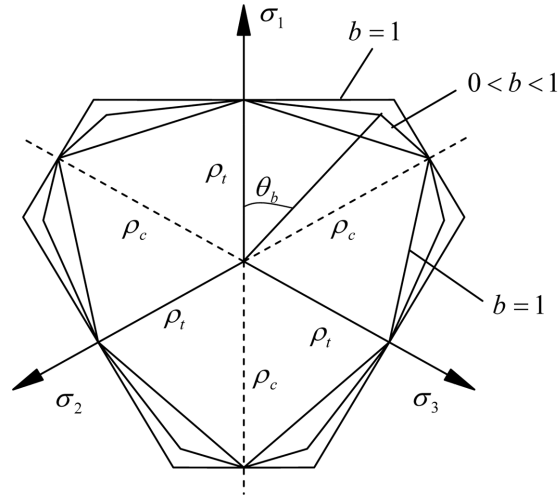Fig. 1 Orthogonal and octahedral twin-shear elements

Fig. 2 Upper- and lower-limit envelope in deviatoric plane based on the UTSS theory

than the strength. The reason can be easily understood that the decreased density of concrete for the same strength level reduces the self-weight, foundation size and construction costs. Furthermore, because the higher porosity of LWA concrete provides a source of water for internal curing of the concrete and provides continued enhancement of cement hydration and compactness, the long term durability of LWA in aggressive environment (e.g., coast or marine environment) was found to even exceed that of normal weight concrete (Tachibana *et al*. 1990, Kayali *et al*. 1999, Zhang and Gjrv 1991). The constitutive equation and strength criterion of LWA concrete play an important role in the application of modern design techniques for reinforced concrete structures, so in the past 20 years a large amount of experimental research has been done on the multi-axial strength and deformation characteristics (Song *et al*. 1996, Song and Wang 2004). Because the strength and deformation behavior of LWA concrete is different from those of normal concrete greatly, the strength criterion established based normal weight concrete cannot fit LWA concrete ideally (Chen 1982). The objective of this paper is to propose a strength criterion for LWA concrete, which can take into account some strength characteristics of LWA concrete under high compressive stress level, to facilitate the application and analysis of LWA concrete structure in complicated project.

2. Strength properties of LWA concrete under triaxial compressive stress

It has been reported that when $\sigma_1/\sigma_3 \geq 0.3$ and $\sigma_2/\sigma_3 \geq 0.5$, a "plastic flow plateau" stage (stress is a constant or has a very slight increase, but strain has a sudden increase) is presented in the principal compressive stress-strain relationships of LWA concrete (Song *et al*. 1996, Liu and Song 2010). After the "plastic flow plateau" stage, the stress continues to increase with the increase of strain, behaving like the characteristic of "stress-intensity" of metal. The mechanism causing this plateau stage is due to the two-step crushing procedure of the inner structure of LWA concrete. At beginning, i.e. during the "plastic flow plateau" stage, the inner structures of LWA concrete have already been destroyed. The failures of mortar frames and lightweight aggregates lead to a large

deformation, so that the stress-strain relationships of LWA concrete presents a "plastic flow plateau" stage. After the stress redistribution, the inner interspaces of LWA concrete specimens are compacted, and then an additional load can be applied on the specimens, like a "stress-intensity" of metal. However, at this stage, the lightweight aggregates and the mortar are already crushed, so that when $\sigma_1/\sigma_3 \geq 0.3$ and $\sigma_2/\sigma_3 \geq 0.5$, the stress of the "plastic flow plateau" stage ought to be the ultimate strength of LWA concrete, but not the peak stress. In addition, the stresses of the "plastic flow plateau" stage are not significantly dependent on the stress ratio (Liu and Song 2010). The stress-strain relationship for a LWA concrete under the confinement of equal lateral stresses is depicted in Fig. 3. Therefore, for the practical application, the ultimate strength surface of LWA concrete should adopt the stress value at which the plastic flow plateau starts. As a result, the ultimate strength surface of LWA concrete grows into a closed spatial curved face intersecting with hydrostatic stress axis at two different points, i.e., the equitriaxial tensile strength point and
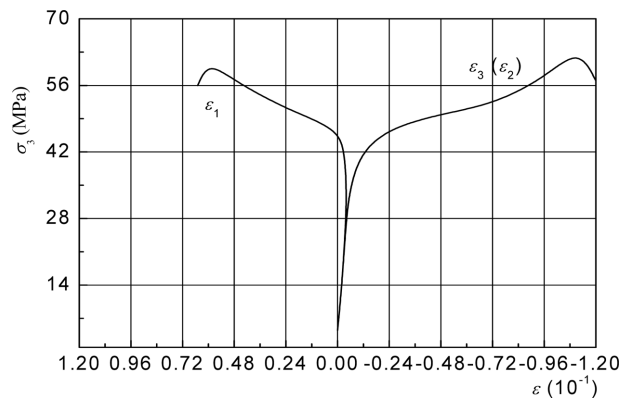

Fig. 3 The stress-strain relationship of LWA concrete under the confinement of equal lateral stresses with a stress ratio of 1:1:0.3
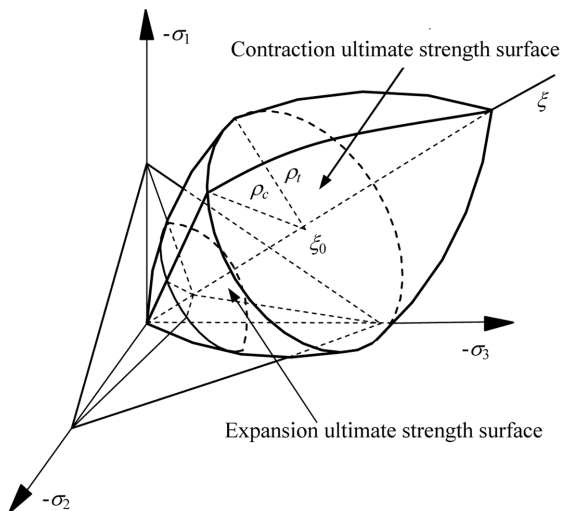

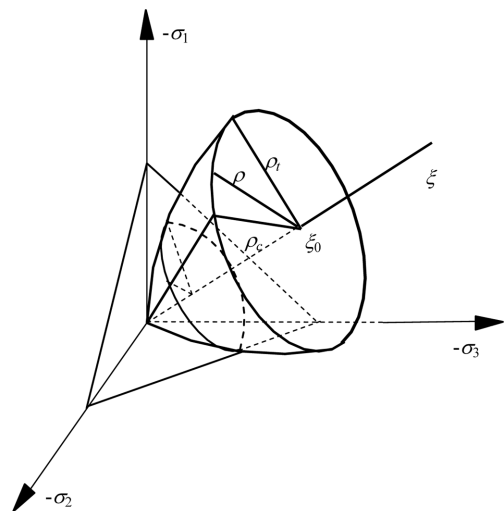Fig. 4 The ultimate strength surface of LWA concrete

Fig. 5 The ultimate strength surface of normal weight concrete

equitriaxial compressive strength point as shown in Fig. 4. Additionally, it can be seen from Fig. 4 that the ultimate strength surface is divided into expansion ultimate strength surface and contraction ultimate strength surface by a deviatoric plane passing through certain hydrostatic stress ξ_0. This characteristic is completely different from that of the normal weight concrete as the ultimate strength surface is open-ended (see Fig. 5).

3. UTSS theory

3.1 Principle of UTSS theory

The UTSS theory is constructed according to the basic orthogonal, octahedral twin-shear element as shown in Fig. 1. The mathematical expression is given as

$$F = \tau_{13} + b\tau_{12} + \beta(\sigma_{13} + b\sigma_{12}) = C \tag{1a}$$

when $\tau_{12} + b\sigma_{12} \geq \tau_{23} + \beta\sigma_{23}$

$$F' = \tau_{13} + b\tau_{23} + \beta(\sigma_{13} + b\sigma_{23}) = C \tag{1b}$$

when $\tau_{12} + b\sigma_{12} < \tau_{23} + \beta\sigma_{23}$.

In Eq. (1a) and (1b), β is a coefficient to reflect the relative effect of the normal stresses; C is a material constant to represent the critical stress state. The principal shear stresses τ_{13}, τ_{12}, τ_{23}, and the corresponding normal stresses σ_{13}, σ_{12}, σ_{23} can be represented by the principal stresses as such:

$$\tau_{13} = \frac{1}{2}(\sigma_1 - \sigma_3), \sigma_{13} = \frac{1}{2}(\sigma_1 + \sigma_3), \tau_{12} = \frac{1}{2}(\sigma_1 - \sigma_2), \sigma_{12} = \frac{1}{2}(\sigma_1 + \sigma_2), \tau_{23} = \frac{1}{2}(\sigma_2 - \sigma_3), \sigma_{23} = \frac{1}{2}(\sigma_2 + \sigma_3).$$

The values of β and C are determined respectively by using the uniaxial tensile strength f_t, the uniaxial compressive strength f_c, as well as the weighting coefficient b as follows

$$\beta = \frac{1 - \alpha}{1 + \alpha} \tag{2}$$

$$C = \frac{1 + b}{1 + \alpha} f_t \tag{3}$$

in which α is the ratio of the uniaxial tensile strength f_t to uniaxial compressive strength f_c, and b is a weighting coefficient that accounts for the relative effect of the intermediate principal shear stress and its corresponding normal stress.

Furthermore, with purpose to denoting the different hydrostatic stress functions of the tensile and compressive meridians of concrete as well as to fitting the various changes of the ultimate envelope in the deviatoric plane, the five-parameter twin-shear strength criterion was proposed (Yu *et al*. 1992). The expression is

$$F = \tau_{13} + b\tau_{12} + \beta(\sigma_{13} + b\sigma_{12}) + A_1\sigma_m + B_1\sigma_m^2 = C \tag{4a}$$

when $0^\circ \leq \theta \leq \theta_b$

$$F' = \tau_{13} + b\tau_{23} + \beta(\sigma_{13} + b\sigma_{23}) + A_2\sigma_m + B_2\sigma_m^2 = C \tag{4b}$$

when $\theta_b \leq \theta \leq 60^\circ$

in which lode angle θ_b is the demarcating angle of the angular point of the trajectory in the deviatoric plane (see Fig. 2); β, A_1, A_2, B_1, B_2, and C are material constants to be determined experimentally; σ_m is the mean stress, i.e., $\sigma_m = (\sigma_1 + \sigma_2 + \sigma_3)/3$.

Rewriting Eq. (4a) and (4b) in terms of the principal stresses σ_1, σ_2, and σ_3 leads to

$$F = \frac{1}{2}(1+b)(1+\beta)\sigma_1 - \frac{b}{2}(1-\beta)\sigma_2 - \frac{1}{2}(1-\beta)\sigma_3 + A_1\sigma_m + B_1\sigma_m^2 = C \tag{5a}$$

when $0^\circ \leq \theta \leq \theta_b$

$$F' = \frac{1}{2}(1+\beta)\sigma_1 + \frac{b}{2}(1+\beta)\sigma_2 - \frac{1}{2}(1+b)(1-\beta)\sigma_3 + A_2\sigma_m + B_2\sigma_m^2 = C \tag{5b}$$

when $\theta_b \leq \theta \leq 60^\circ$

If the principal stresses in Eq. (5a) and (5b) are represented by the stress invariants I_1, J_2, and lode angle θ, the following expressions can be obtained

$$F = (1+b)(3+\beta)\sqrt{\frac{J_2}{3}}\cos\theta + (1-\beta)(1-b)\sqrt{J_2}\sin\theta + 2\beta(1+b)\frac{I_1}{3} + 2A_1\left(\frac{I_1}{3}\right) + 2B_1\left(\frac{I_1}{3}\right)^2 = 2C \tag{6a}$$

when $0^\circ \leq \theta \leq \theta_b$

$$F' = (3+\beta-2b\beta)\sqrt{\frac{J_2}{3}}\cos\theta + (1-\beta+2b)\sqrt{J_2}\sin\theta + 2\beta(1+b)\frac{I_1}{3} + 2A_2\left(\frac{I_1}{3}\right) + 2B_2\left(\frac{I_1}{3}\right)^2 = 2C \tag{6b}$$

when $\theta_b \leq \theta \leq 60^\circ$

In general, the Haigh-Westergaard coordinates (ξ, ρ, and θ) are used to simply the expression of Eq. (6a) and (6b). As a result, Eq. (6a) and (6b) can be written by the following

$$(1+b)(3+\beta)\frac{\rho}{\sqrt{2}}\cos\theta + \sqrt{3}(1-b)(1-\beta)\frac{\rho}{\sqrt{2}}\sin\theta + f_1(\xi) = 0 \tag{7a}$$

when $0^\circ \leq \theta \leq \theta_b$

$$(3+\beta-2b\beta)\frac{\rho}{\sqrt{2}}\cos\theta + \sqrt{3}(1+2b-\beta)\frac{\rho}{\sqrt{2}}\sin\theta + f_2(\xi) = 0 \tag{7b}$$

when $\theta_b \leq \theta \leq 60^\circ$, where $f_1(\xi)$ and $f_2(\xi)$ are the second-order polynomials of the hydrostatic stress coordinate ξ as follows

$$f_1(\xi) = -2\sqrt{3}C + 2[\beta(1+b) + A_1]\xi + \frac{2}{\sqrt{3}}B_1\xi^2 \tag{8a}$$

$$f_2(\xi) = -2\sqrt{3}C + 2[\beta(1+b) + A_2]\xi + \frac{2}{\sqrt{3}}B_2\xi^2 \tag{8b}$$

By dividing the uniaxial compressive strength of concrete on both sides of Eq. (7a) and (7b), they will be non-dimensionalized as the following forms

$$\bar{\rho} = -\frac{\sqrt{2}f_1(\xi)}{f_c[(1+b)(3+\beta)\cos\theta + \sqrt{3}(1-b)(1-\beta)\sin\theta]} \tag{9a}$$

when $0^\circ \leq \theta \leq \theta_b$

$$\bar{\rho} = -\frac{\sqrt{2}f_2(\xi)}{f_c[(3+\beta(1-2b))\cos\theta + \sqrt{3}(1-\beta+2b)\sin\theta]} \tag{9b}$$

when $\theta_b \le \theta \le 60^o$.

3.2 Application of UTSS to LWA concrete

Eq. (9a) and (9b) are functions representing the ultimate strength envelope of LWA concrete based on the UTSS. By letting $\theta = 0^o$ and $\theta = 60^o$ respectively, the expressions of tensile and compressive meridians can be obtained as follows

$$\bar{\rho}_t = -\frac{\sqrt{2}f_1(\xi)}{f_c(1+b)(3+\beta)} \qquad (\theta=0^o) \tag{10a}$$

$$\rho_c = -\frac{\sqrt{2}f_2(\xi)}{f_c(1+b)(3-\beta)} \qquad (\theta=60^o) \tag{10b}$$

Combining Eq. (10a) and (10b) with Eq. (9a) and (9b) leads to

$$\bar{\rho} = \frac{(1+b)(3+\beta)\bar{\rho}_t}{(1+b)(3+\beta)\cos\theta + \sqrt{3}(1-b)(1-\beta)\sin\theta} \tag{11a}$$

when $0^o \le \theta \le \theta_b$

$$\bar{\rho} = \frac{(1+b)(3-\beta)\bar{\rho}_c}{[3+\beta(1-2b)]\cos\theta + \sqrt{3}(1+2b-\beta)\sin\theta} \tag{11b}$$

when $\theta_b \le \theta \le 60^o$.

It is obviously observed that the ultimate strength envelope expressed by Eq. (11a) and (11b) can be determined by linearly interpolating operation between the compressive meridian $\bar{\rho}_c$ and tensile meridian $\bar{\rho}_t$.

Since $f_1(\xi)$ and $f_2(\xi)$ are the second-order polynomials, Eq. (10a) and (10b) for the compressive and tensile meridians $\bar{\rho}_c$ and $\bar{\rho}_t$ can be expressed in an equivalent quadratic form as

$$\bar{\rho}_t = m_0 + m_1\bar{\xi} + m_2\bar{\xi}^2 \qquad (\theta=0^o) \tag{12a}$$

$$\bar{\rho}_c = n_0 + n_1\bar{\xi} + n_2\bar{\xi}^2 \qquad (\theta=60^o) \tag{12b}$$

where m_0, m_1, m_2, and n_0, n_1, n_2 are constants. Their explicit expressions can be easily derived by comparing Eq. (12a) and (12b) with Eq. (10a) and (10b) as follows

$$\begin{cases} m_0 = \dfrac{2\sqrt{6}C}{(1+b)(3+\beta)f_c} \\[3mm] m_1 = -\dfrac{2\sqrt{2}[(1+b)\beta+A_1]}{(1+b)(3+\beta)} \\[3mm] m_2 = -\dfrac{2\sqrt{2}B_1f_c}{\sqrt{3}(1+b)(3+\beta)} \end{cases} \tag{13a}$$

$$\begin{cases} n_0 = \dfrac{2\sqrt{6}C}{(1+b)(3-\beta)f_c} \\[3mm] n_1 = -\dfrac{2\sqrt{2}[(1+b)\beta + A_2]}{(1+b)(3-\beta)} \\[3mm] n_2 = -\dfrac{2\sqrt{2}B_2 f_c}{\sqrt{3}(1+b)(3-\beta)} \end{cases} \tag{13b}$$

Concerning the basic role of the compressive and tensile meridians in the strength criterion, a few certain characteristic strengths are firstly selected and will be used to determine the values of the constants in Eq. (12a) and (12b). For LWA concrete material, the characteristic strengths are the uniaxial tensile strength f_t ($\theta = 0°$), uniaxial compressive strength f_c ($\theta = 60°$), equibiaxial compressive strength f_{bc} ($\theta = 60°$) as well as the strengths at the couple intersections of the compressive and tensile meridians, i.e., the two intersecting points of the ultimate envelope with the hydrostatic stress axis. In general, the strength values on these characteristic points can be easily available through experiments.

Let $\alpha = f_t/f_c$, $\bar{\alpha} = f_{bc}/f_c$, and suppose the coordinates of the intersections of the tensile and compressive meridians with the hydrostatic stress axis are $\bar{\xi}_t$ and $\bar{\xi}_c$, which are respectively under the equitriaxial tensile and equitriaxial compressive states. In addition, the positions of the characteristic strength points can be calculated through relationships between the normalized Haigh-Westergaard coordinate ($\bar{\xi}, \bar{\rho}, \theta$) and the three principal stresses.

As a result, the three characteristic strength points required for construction of the tensile meridian are obtained in the normalized Haigh-Westergaard coordinate system ($\bar{\xi}, \bar{\rho}, \theta$) as follows:

(1) $\left(\dfrac{\alpha}{\sqrt{3}}, \sqrt{\dfrac{2}{3}}\alpha, 0° \right)$ for uniaxial tensile strength;

(2) $\left(-\dfrac{2\bar{\alpha}}{\sqrt{3}}, \sqrt{\dfrac{2}{3}}\bar{\alpha}, 0° \right)$ for equibiaxial compressive strength;

(3) $(\bar{\xi}_c, 0, 0°)$ for equitriaxial compressive strength at the intersection of compressive meridian with hydrostatic stress axis.

Substituting them into Eq. (13a) respectively yields three simultaneous equations, from which the expressions for the coefficients of the tensile meridian can be derived as

$$m_0 = \frac{\sqrt{2}\,\alpha\bar{\alpha}[(\alpha - 4\bar{\alpha})\bar{\xi}_c - 3\sqrt{3}\,\bar{\xi}_c^2]}{(2\bar{\alpha} + \sqrt{3}\,\bar{\xi}_c)(\alpha - \sqrt{3}\,\bar{\xi}_c)(\alpha + 2\bar{\alpha})} \tag{14a}$$

$$m_1 = \frac{\sqrt{2}\,[\alpha\bar{\alpha}((4\bar{\alpha} - \alpha) + (\bar{\alpha} - \alpha)\bar{\xi}_c^2)]}{(2\bar{\alpha} + \sqrt{3}\,\bar{\xi}_c)(\alpha - \sqrt{3}\,\bar{\xi}_c)(\alpha + 2\bar{\alpha})} \tag{14b}$$

$$m_2 = \frac{3\sqrt{2}\,[\sqrt{3}\,\alpha\bar{\alpha} + (\alpha - \bar{\alpha})\bar{\xi}_c]}{(2\bar{\alpha} + \sqrt{3}\,\bar{\xi}_c)(\alpha - \sqrt{3}\,\bar{\xi}_c)(\alpha + 2\bar{\alpha})} \tag{14c}$$

For the compressive meridian, the Haigh-Westergaard coordinates of the three corresponding characteristic strength points are as follows:

(1) $\left(-\dfrac{1}{\sqrt{3}}, \sqrt{\dfrac{2}{3}}, 60^{\circ}\right)$ for uniaxial compressive strength;

(2) $(\overline{\xi}_c, 0, 60^{\circ})$ for equitriaxial compressive strength at the intersection of compressive meridian with hydrostatic stress axis;

(3) $(\overline{\xi}_t, 0, 60^{\circ})$ for equitriaxial tensile strength at the intersection of compressive meridian with hydrostatic stress axis, and $\overline{\xi}_t$ can be calculated by Eq. (13a) as $\overline{\xi}_t = -m_1 - \sqrt{m_1^2 - 4m_0 m_2}/2m_2$.

With the same method mentioned above, the coefficients of the compressive meridian are expressed as

$$n_0 = \frac{\sqrt{6}\,\overline{\xi}_t\overline{\xi}_c}{(\sqrt{3}\,\overline{\xi}_c + 1)(\sqrt{3}\,\overline{\xi}_t + 1)} \tag{15a}$$

$$n_1 = -\frac{\sqrt{6}(\overline{\xi}_t + \overline{\xi}_c)}{(\sqrt{3}\,\overline{\xi}_c + 1)(\sqrt{3}\,\overline{\xi}_t + 1)} \tag{15b}$$

$$n_2 = -\frac{\sqrt{6}}{(\sqrt{3}\,\overline{\xi}_c + 1)(\sqrt{3}\,\overline{\xi}_t + 1)} \tag{15c}$$

Based on Eq. (16), it is apparent that $\dfrac{m_0}{n_0} = \dfrac{3 - \beta}{3 + \beta}$, thus one can has

$$\beta = \frac{3(n_0 - m_0)}{n_0 + m_0} \tag{16}$$

By equating the right-hand sides of the two equations in Eq. (8), the lode angle θ_b can be easily derived as

$$\theta_b = \arctan = \frac{(3 + \beta)[\overline{\rho}_t(3 + \beta - 2b\beta) - \overline{\rho}_c(1 + b)(3 - \beta)]}{\sqrt{3}[\overline{\rho}_c(3 - \beta)(1 - b)(1 - \beta) - \overline{\rho}_t(3 + \beta)(1 + 2b - \beta)]} \tag{17}$$

in which the value of β is determined by Eq. (16).

4. Construction of the criterion by experimental results

4.1 Tensile and compressive meridians

The multi-axial test data on LWA concrete from Song *et al.* (1996) are used to quantify the coefficients in the ultimate strength model represented from Eq. (11a) to Eq. (12b). In the test, the specimens of 100 mm × 100 mm × 100 mm cubes were cast in steel molds. The lytag with a round shape was used as coarse aggregate. An ordinary Portland cement 42.5R (Type CEM I) based on Chinese code was used as the binding material. The proportion of mixture was designed as 1:0.42:1.22:0.98 for composition of the Portland cement, water, sand and lytag, with a water-to-cement ratio of 0.42. The experimental results of multi-axial strength, as well as their coordinates in the Haigh-Westergaard coordinate system are listed in Table 1, in which only the principal stresses

Table 1 Multi-axial strengths of LWA concrete and values in Haigh-Westergaard coordinate system

No.	σ_1 (MPa)	σ_2 (MPa)	σ_3 (MPa)	σ_{oct} (MPa)	τ_{oct} (MPa)	ξ (MPa)	ρ (MPa)	θ (°)
1	-2.82	-2.82	-28.17	-11.27	11.95	-19.52	20.70	60
2	-3.15	-7.87	-31.49	-14.17	12.40	-24.54	21.47	51.06
3	-3.10	-9.30	-31.00	-14.47	11.96	-25.06	20.72	47.78
4	-3.42	-17.08	-34.15	-18.22	12.57	-31.55	21.77	33.67
5	-3.18	-23.85	-31.80	-19.61	12.06	-33.97	20.89	15.61
6	-3.03	-30.32	-30.32	-21.22	12.86	-36.76	22.28	0
7	-11.30	-13.56	-45.19	-23.35	15.47	-40.44	26.80	56.58
8	-12.08	-24.16	-48.31	-28.18	15.06	-48.81	26.09	40.89
9	-10.98	-32.93	-43.90	-29.27	13.69	-50.70	23.71	19.10
10	-9.77	-39.09	-39.09	-29.32	13.82	-50.78	23.94	0
11	-15.20	-15.20	-50.66	-27.02	16.72	-46.80	28.95	60
12	-15.32	-25.53	-51.05	-30.63	15.03	-53.06	26.03	43.90
13	-14.21	-47.38	-47.38	-36.32	15.64	-62.91	27.08	0
14	-29.43	-29.43	-58.86	-39.24	13.87	-67.97	24.03	60
15	-25.74	-38.60	-51.47	-38.60	10.50	-66.86	18.19	30.01
16	-25.66	-51.31	-51.31	-42.76	12.09	-74.06	20.94	0
17	-41.96	-41.96	-55.94	-46.62	6.59	-80.75	11.41	60
18	-38.03	-50.70	-50.70	-46.48	5.97	-80.50	10.35	0
19	-57.74	-57.74	-57.74	-57.74	0	-100.01	0	NAN
20	0.90	0.09	-0.90	0.03	0.74	0.052	1.27	33.30
21	0.86	0.15	-1.15	-0.05	0.83	-0.08	1.44	39.62
22	0.65	0.13	-1.30	-0.17	0.82	-0.30	1.43	45.08
23	0.41	0.21	-4.10	-1.16	2.08	-2.01	3.60	57.75
24	0.60	0.60	-0.80	0.13	0.66	0.23	1.14	60.00
25	0.58	0.58	-2.30	-0.38	1.36	-0.66	2.35	60.00
26	0.71	-2.84	-2.84	-1.66	1.67	-2.87	2.90	0
27	1.97	-2.62	-2.62	-1.09	2.16	-1.89	3.75	0
28	1.72	-1.72	-1.72	-0.57	1.62	-0.99	2.81	0
29	1.75	1.75	1.75	1.75	0	3.03	0	NAN
30	1.23	0.62	0.62	0.82	0.29	1.43	0.50	0
31	1.84	0.46	0.46	0.92	0.65	1.59	1.13	0
32	0	-5.25	-20.98	-8.74	8.91	-15.14	15.44	46.09
33	0	-10.28	-20.56	-10.28	8.39	-17.81	14.54	30
34	0	-15.06	-20.08	-11.71	8.53	-20.29	14.78	13.90
35	0	-21.35	-21.35	-14.23	10.06	-24.65	17.43	0
36	0.48	0	-9.69	-3.07	4.69	-5.32	8.11	57.60
37	1.25	0	-4.99	-1.25	2.70	-2.16	4.67	49.09
38	0.63	0	-6.33	-1.90	3.14	-3.29	5.44	55.31
39	1.80	0	-3.60	-0.6	2.24	-1.04	3.89	40.89
40	1.98	0	-2.64	-0.22	1.89	-0.38	3.28	34.72
41	1.72	0	-1.72	0	1.40	0	2.43	30

of σ_1, σ_2, and σ_3 are measured through the experiment.

From Table 1, it is found that for $\sigma_1 = \sigma_2$, when the equal lateral stresses are $0.1\sigma_3$, $0.25\sigma_3$ and $0.3\sigma_3$, the strength values of σ_3 are 1.69, 2.52 and 3.04 times of the uniaxial compressive strength respectively; when the equal lateral stresses are $0.5\sigma_3$, $0.75\sigma_3$, $1.0\sigma_3$, the strength values of σ_3 are 3.53, 3.35 and 3.46 times of the uniaxial compressive strength respectively (Song *et al*. 1996). This phenomenon denotes the strength characteristics of LWA concrete under triaxial stress state: when
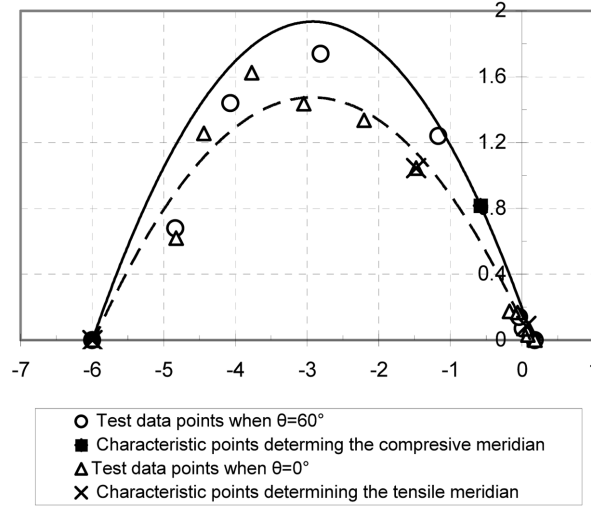
Fig. 6 Tensile and compressive meridians based on the UTSS theory and experimental results

the lateral compressive stress is less than a critical value, e.g., $\sigma_1/\sigma_3 = 0.38$, as mentioned in Song *et al.* (1996), an increase of confinement results in an increase of the ultimate strength of σ_3; however, when the lateral compressive stress is higher than the critical value, the ultimate strength of σ_3 approximately approaches to a constant, in other words, there exhibits the "plastic flow plateau" phenomenon, which can be attributed to the crushing of coarse aggregate under high confinement. Therefore, the strength will not increase with the increase of the lateral compressive stress.

Additionally, the uniaxial tensile strength f_t, the uniaxial compressive strength f_c, and the equibiaxial compressive f_{bc} have also been obtained as 1.75 MPa, 16.68 MPa and 31.35 MPa, respectively. Therefore, the constants α and $\overline{\alpha}$ can be determined as $\alpha = f_t/f_c = 1.75/16.68 = 0.1049$, $\overline{\alpha} = f_{bc}/f_c = 1.280$. From Table 1, one can find that the intersection point coordinate of the tensile meridian with compressive hydrostatic stress axis is $\overline{\xi}_c = \xi_c/f_c = -100.01/16.68 = -5.9958$. After substituting these three values into Eq. (14a) to (14c), it yields: $m_0 = 0.1362$, $m_1 = -0.8237$, $m_2 = -0.1411$. Subsequently, the intersection point coordinate of the compressive meridian with tensile hydrostatic stress axis can be calculated as $\overline{\xi}_t = -m_1 - \sqrt{m_1^2 - 4m_0 m_2}/2m_2 = 0.1607$. Then from Eq. (15a) to (15c), the coefficients of compressive meridian equation can be determined as $n_0 = 0.1968$, $n_1 = -1.1913$, $n_2 = -0.2042$. Finally, the parameter of β is calculated from Eq. (16) as $\beta = 0.5459$.

Fig. 6 shows the comparison between the tensile and compressive meridians based on the UTSS theory and the experimental results, which indicates a good agreement. And more significantly, the plastic flow plateau of LWA concrete under high compressive stress is represented since the tensile and compressive meridians intersect with the hydrostatic axis at two common points. This behavior is completely different from that of normal concrete as the ultimate strength surface of the latter is open-ended.

4.2 Ultimate strength envelope in the deviatoric plane

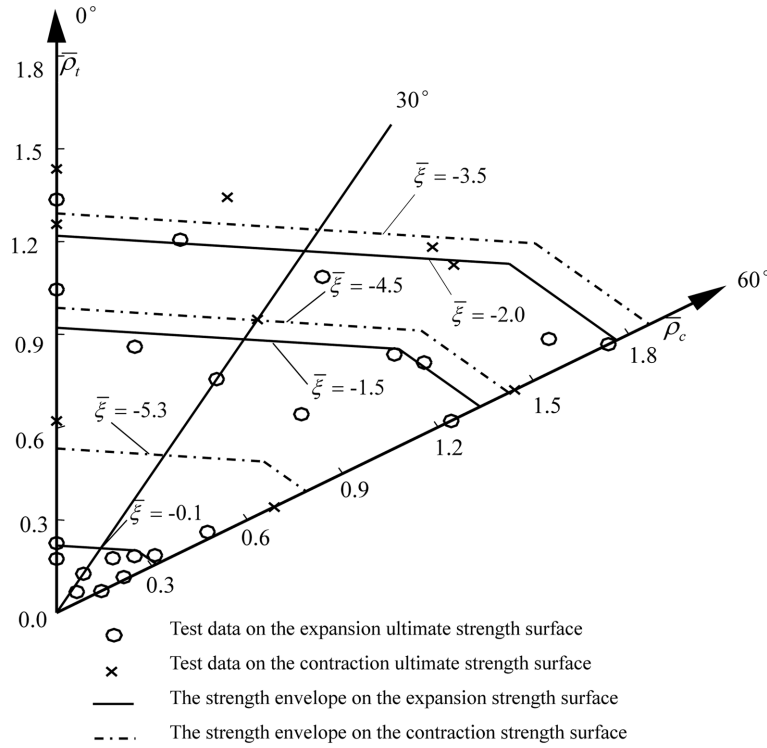The test data in Table 1 are plotted in the deviatoric plane as shown in Fig. 7. The ultimate

Fig. 7 The ultimate strength envelope in deviatoric plane under different hydrostatic stress

strength envelopes represented by Eq. (11a) and (11b) under different hydrostatic stress levels are also depicted in Fig. 7. It should be pointed out that in the present paper, the value of weighting coefficient b is arbitrarily set as 1/2 although it can be taken other values in its range from 0 to 1. Because b only influences the shape of the ultimate strength envelope on the deviatoric plane, its values may be possibly obtained when sufficient test data are available. Since the ultimate strength surface of LWA concrete is divided into two parts, i.e., the expansion ultimate strength surface and the contraction ultimate strength surface, it can be observed that at the initial stage, the ultimate strength envelope in the deviatoric plane enlarges with the increase of hydrostatic stress $\bar{\xi}$, and then, the strength envelope begins to contract when $\bar{\xi}$ is lager than a certain value (based the test data in this paper, this critical value of $\bar{\xi}$ is −2.9189). In other words, the non-dimensionalized radius $\bar{\rho}$ of ultimate strength envelope in the deviatoric plane increases with the increase of hydrostatic stress $\bar{\xi}$ when $\bar{\xi} \geq -2.9189$, but decreases with the increase of hydrostatic stress $\bar{\xi}$ when $\bar{\xi} < 2.9189$.

5. Conclusions

Based on the Unified Twin-Shear Strength (UTSS) theory proposed by Prof. Yu (Yu *et al.* 1992) and with help of the experimental results, a multi-axial strength criterion in terms of LWA concrete is developed, which is able to represent the "plastic flow plateau" phenomenon of LWA concrete

under high compressive stress. The principle characteristics of the present strength criterion can be stated as follows:

(1) The mathematical formulation of this strength criterion represents the clear physical concept and a simple mechanical form, which can be easily realized in the engineering applications.

(2) This criterion can reflect the characteristic of "plastic flow plateau" of LWA concrete under high compressive stress, and especially the ultimate strength surface having a transition from an expansion tendency to the contraction process.

(3) The parameters in the criterion can be determined with a few characteristic stress points, i.e., the uniaxial tensile strength f_t, the uniaxial compressive strength f_c, and the equibiaxial compressive f_{bc}, which will be easily obtained from test.

Acknowledgements

References

Alduaij, J., Alshaleh, K., Haque, M.N. and Ellaithy, K. (1999), "Lightweight concrete in hot coastal areas", *Cement Concrete Compos.*, **21**(5), 453-458.

Chen, W.F. (1982), *Plasticity in Reinforced Concrete*, Mcgraw-Hill, New York.

Ergul, Y., Cengiz, D.A. and Alaettin, K. (2003), "Strength properties of lightweight concrete made with basaltic pumice and fly ash", *Mater. Lett.*, **57**(15), 2267-2270.

Fan, S.C. and Wang, F. (2002), "A new strength criterion for concrete", *ACI Struct. J.*, **99**(3), 317-326.

Haug, A.K. and Fjeld, S. (1996), "A float concrete platform hull made of lightweight aggregate concrete", *Eng. Struct.*, **18**(11), 831-836.

Imran, I. and Pantazopoulou, S.J. (1996), "Experimental study of plain concrete under triaxial stress", *ACI Mater. J.*, **93**(6), 589-601.

Jo, B.W., Park, S.K. and Park, J.B. (2007), "Properties of concrete made with alkali-activated fly ash lightweight aggregate (AFLA)", *Cement Concrete Compos.*, **29**(2), 128-135.

Kayali, O., Haque, M.N. and Zhu, B. (1999), "Drying shrinkage of fibre-reinforced lightweight aggregate concrete containing fly ash", *Cement Concrete Res.*, **29**(11), 1835-1840.

Kupfer, H., Hilsdorf, H.K. and Rusch, H. (1969), "Behavior of concrete under biaxial stresses", *J. ACI*, **66**(8), 656-666.

Liu, H.Y. and Song, Y.P. (2010), "Experimental study of lightweight aggregate concrete under multiaxial stresses",. *J. Zhejiang University-SCIENCE A (Applied Physics & Engineering)*, **11**(8), 545-554.

Melby, K., Jordet, E.A. and Hansvold, C. (1996), "Long-span bridges in Norway constructed in high-strength LWA concrete", *Eng. Struct.*, **18**(11), 845-849.

Menétrey, P. and Willam, K.J. (1995), "Triaxial failure criterion for concrete", *ACI Struct. J.*, **92**(3), 311-318.

Rossignolo, J.A., Agnesini, M.V.C. and Morais, J.A. (2003), "Properties of high-performance LWAC for precast structures with Brazilian lightweight aggregates", *Cement Concrete Compos.*, **25**(1), 77-82.

Song, Y.P. (2002), "Constitutive model and failure criterion of multiple concrete materials", Hydraulic and

Hydroelectricity Press, Beijing, China.

Song, Y.P., Song, X. and Feng, S. (2000), "Temperature and stress analysis of an experimental model prestressed lightweight concrete platform", *China Ocean Eng.*, **14**(3), 279-288.

Song, Y.P. and Wang, L. (2004), "A four-parameter multi-axial strength criterion for lightweight aggregate concrete", *Proceeding of the 6th ISOPE/Asia Offshore Mechanics Symposium,* Vladivostock, September.

Song, Y.P., Zhao, G.F., Peng, F. and Shen, J.N. (1996), "Strength of lightweight concrete under triaxial compression", *China Ocean Eng.*, **10**(2), 239-244.

Tachibana, D., Imai, M. and Okada, T. (1990), "Qualities of high-strength lightweight concrete used for construction of arctic offshore platform", *J. Off. Mech. Arc. Eng.*, **112**(1), 27-34.

Traina, L.A. and Mansour, S. (1991), "Biaxial strength and deformational behavior of plain and steel fiber concrete", *ACI Mater. J.*, **88**(4), 354-362.

Wang, C.Z., Guo, Z.H. and Zhang, X.Q. (1987), "Experimental investigation of biaxial and triaxial compressive concrete strength", *ACI Mater. J.*, **84**(2), 92-100.

Yu, M.H., He, L.N. and Liu, C.Y. (1992), "Twin shear unified yield criterion and its application", *Scientific Bulletin*, **37**(2), 182-185.

Zhang, M.H. and Gjrv, O.E. (1991), "Mechanical properties of high-strength lightweight concrete", *ACI Mater. J.*, **88**(3), 240-247.